UCRL-JC-124508
PREPRINT

Improved Beam Smoothing with SSD using Generalized Phase Modulation

J. E. Rothenberg

**This paper was prepared for submittal to the
2nd Annual International Conference on
Solid-State Lasers for Application to ICF
Paris, France
October 22-25, 1996**

January 8, 1997

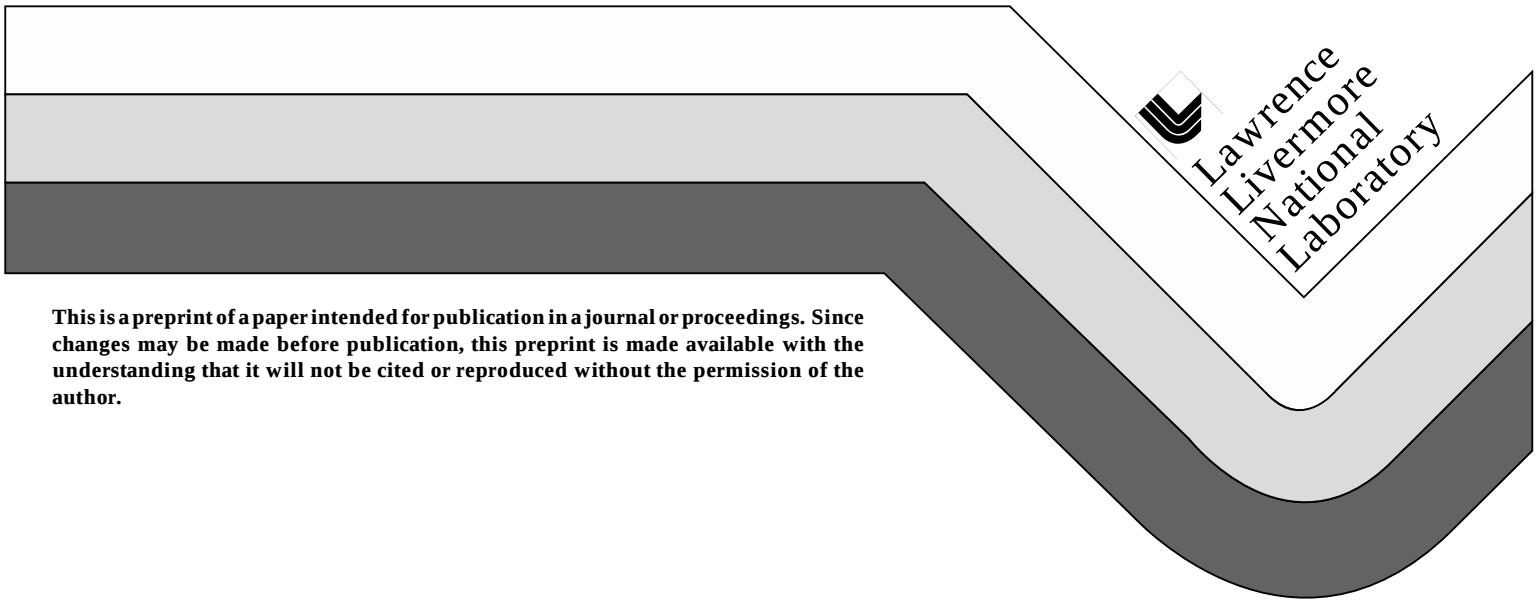

This is a preprint of a paper intended for publication in a journal or proceedings. Since changes may be made before publication, this preprint is made available with the understanding that it will not be cited or reproduced without the permission of the author.

DISCLAIMER

This document was prepared as an account of work sponsored by an agency of the United States Government. Neither the United States Government nor the University of California nor any of their employees, makes any warranty, express or implied, or assumes any legal liability or responsibility for the accuracy, completeness, or usefulness of any information, apparatus, product, or process disclosed, or represents that its use would not infringe privately owned rights. Reference herein to any specific commercial product, process, or service by trade name, trademark, manufacturer, or otherwise, does not necessarily constitute or imply its endorsement, recommendation, or favoring by the United States Government or the University of California. The views and opinions of authors expressed herein do not necessarily state or reflect those of the United States Government or the University of California, and shall not be used for advertising or product endorsement purposes.

Improved Beam Smoothing with SSD using Generalized Phase Modulation

Joshua E. Rothenberg

Lawrence Livermore National Laboratory, L-439
P. O. Box 808, Livermore, CA 94551
Phone: (510) 423-8613, FAX: (510) 422-5537
email: JR1 @ LLNL.GOV

ABSTRACT

The smoothing of the spatial illumination of an inertial confinement fusion target is examined by its spatial frequency content. It is found that the smoothing by spectral dispersion method, although efficient for glass lasers, can yield poor smoothing at low spatial frequency. The dependence of the smoothed spatial spectrum on the characteristics of phase modulation and dispersion is examined for both sinusoidal and more general phase modulation. It is shown that smoothing with non-sinusoidal phase modulation can result in spatial spectra which are substantially identical to that obtained with the induced spatial incoherence or similar method where random phase plates are present in both methods and identical beam divergence is assumed.

Keywords: Beam smoothing, smoothing by spectral dispersion, inertial confinement fusion.

1. INTRODUCTION

A number of methods have been pursued to achieve the high degree of target illumination uniformity required to minimize seeding of Rayleigh-Taylor instabilities[1] in the direct drive approach to inertial confinement fusion (ICF).[2-14] The use of spatially incoherent light[2] (referred to as the induced spatial incoherence method or ISI) imaged[4] onto the target requires amplification of a highly nonuniform spatial and temporal intensity distribution, which is suitable for gaseous amplifier media. This method has been extended to glass lasers using both multimode fibers[5,9] and spectral dispersion[8] as the spatially incoherent sources, and termed as a partially coherent light (PCL)[9] or an amplified spontaneous emission (ASE)[8] source. However, the lack of intensity uniformity of spatially incoherent light in glass amplifiers results in a large decrease in efficiency.[7] An alternative approach which is well suited to glass lasers is that of smoothing by spectral dispersion (SSD),[6] where the coherence is reduced by spectrally dispersing a frequency modulated (FM) beam and a random phase plate (RPP)[3] is used to control the precise focused envelope of the speckled intensity on the target. In the SSD method, because only phase modulation is imposed, the intensity uniformity of the near field beam can be maintained and hence efficient use is made of the amplifiers. The SSD method can be made more effective by phase modulating the beam again after dispersion, and

dispersing a second time in a direction orthogonal to the first dispersion (2D-SSD).[10] It has been shown that in the usual implementation of (1D or 2D) SSD, where sinusoidal phase modulation (FM) is used, one can obtain poor smoothing of low spatial frequency nonuniformities.[11] However, calculations indicate that the aggregate smoothing rate (i.e. when integrated over all spatial frequencies) obtained with SSD can be improved by using non sinusoidal phase modulation.[12] This approach was implemented by using random phase modulation (RPM) in an optical fiber and did demonstrate improved aggregate smoothing.[13,14] However, because of the strong spatial frequency dependence of the Rayleigh-Taylor gain and other physics of the direct drive target, the aggregate smoothing rate is insufficient to characterize smoothing performance, and it is critical to understand the smoothing behavior as a function of spatial frequency for the gamut of available smoothing methods.[11]

In this paper it is shown that the SSD method can achieve smoothing equivalent to the ISI method (or PCL, for brevity this method shall simply be referred to as ISI hereafter) by applying RPM or appropriate non-sinusoidal phase modulation with adequate angular dispersion, when a similar RPP is used in both methods. Standard SSD employs sinusoidal phase modulation (FM) and spectral dispersion such that the instantaneous frequency cycles across the beam ("color cycling"). As was originally discussed by Skupsky et al,[6] increasing the dispersion to generate many color cycles yields proportionally better smoothing at low spatial frequency. However, coherences between the colors distributed across the beam, owing to the pure periodic nature of the phase, leads to reduced smoothing at particular spatial frequencies. By using non-sinusoidal phase modulation, these resonances can be eliminated and smoothing at low spatial frequency equivalent to that of the random ISI method can be obtained.

The technique of SSD utilizing generalized phase modulation is depicted in Fig. 1. The beam is modulated with some phase function $\phi(t)$ and then dispersed by a grating before amplification. The effect of the dispersion is to time skew the phase function across the beam. I.e., the phase after dispersion is described by $\phi(t - sx)$, where the time skew per unit distance s is proportional to the grating dispersion.[15] The grating preceding the modulator is oriented with opposite dispersion (skew) to pre compensate for the second grating such that the input temporal envelope $E_{in}(t)$ is undistorted. For 2D SSD a second sequence of orthogonal gratings and an incommensurate modulator are added.[10,12] A random phase plate (RPP) is used to control the envelope of the speckled illumination on the target.

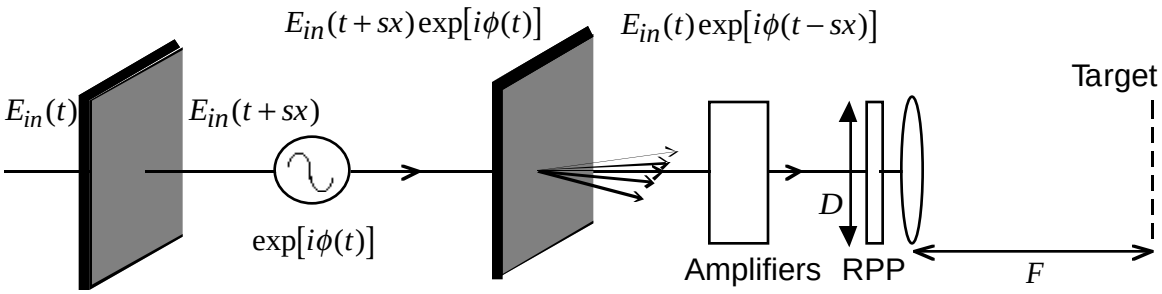

Figure 1: Schematic layout of 1D-SSD with generalized phase modulation.

For a completely randomized smoothing method (e.g. ISI with a very large beam divergence), where the speckle patterns at successive coherence times are random over all spatial frequencies of interest, one ideally finds that all spatial frequencies are smoothed at the same bandwidth limited rate. For a realistic smoothing method, however, the extent of the speckle motion is limited and therefore there will always be a low spatial frequency limit below which no smoothing occurs. For ease of comparison the SSD and (modified) ISI methods are compared based upon equal laser divergence FWHM, with RPP's present. For completeness, the results for ideal ISI (i.e., with divergence much larger than the aberrations of the amplifier and the RPP absent) are also presented in the calculations. In all calculations presented here the RPP is taken to produce a far field spot much larger than the beam motion associated with the smoothing source, and much larger than any spatial wavelengths considered.

2. SMOOTHING BY THE RANDOM ISI METHOD

The behavior of the ISI smoothing method is illustrated in Fig. 2, where the spatial power spectra of the integrated intensity on target vs. normalized spatial frequency are shown at a series of integration times (solid curves). In these calculations the time varying speckle pattern is calculated by taking the near field at the final focus lens to be the product of a static random binary pattern (for the RPP) and a time varying random phase pattern with a Gaussian angular spread of FWHM of $50\lambda / D$. The far field intensities at successive time steps are calculated by Fourier Transform and integrated to obtain the fluence. The squared magnitude of the Fourier Transform of the far field fluence then yields the spatial power spectra presented. In all the calculations presented here a square uniform near field beam of width D is assumed.

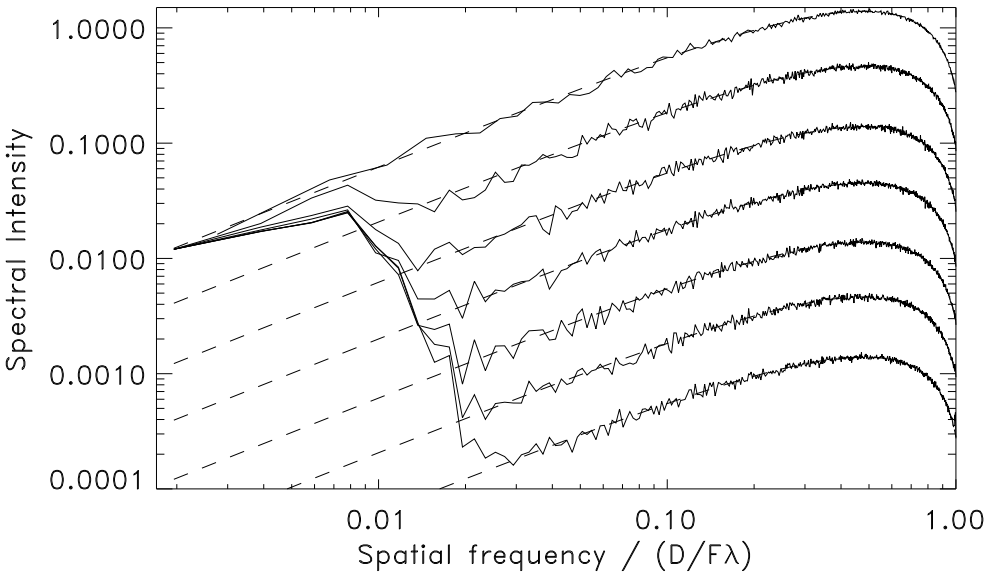

Figure 2: Calculated spatial spectral intensity of speckle patterns with random smoothing (ISI) of divergence FWHM 50 λ / D for (top to bottom curves) the initial static speckle pattern

and after an integration time equivalent to 3, 10, 30, 100, 300, and 1000 coherence times. The dashed lines show the ideal smoothing result for the case of large beam divergence.

The spatial frequency scale shown is normalized to the F# limited spatial frequency $f_0 \equiv D/\lambda F$, where F is the final lens focal length, and λ is the wavelength on target (see Fig. 1). For example, in the proposed National Ignition Facility (NIF) focusing geometry (D = 35 cm, F = 7 m, λ = 0.35 μm) λ / D = 1 μrad, f_0 corresponds to a wavelength of 7 μm, and for a direct drive target of radius r = 1.6 mm, f_0 corresponds to an l-mode of $2\pi r f_0 = 1500$. These spectra have been integrated over azimuth in the spectral plane (f_x, f_y) so that they are only dependent on the magnitude of the spatial frequency f (or l-mode), and are scaled such that the integral over the normalized spatial frequency yields the normalized variance of the target fluence. Thus, the spectral intensity $S(f)$ shown is defined to such that $\int S(f)df \equiv \sigma^2$. In particular, for a static speckle pattern (e.g., top curve in Fig. 2) which has unity variance,[16] one sees that $\int S(f)df = 1$.

The dashed curves in Fig. 2 show the ideal behavior of ISI smoothing of unlimited beam divergence, and as described above are simply given by the initial static speckle spectrum divided by the number of coherence times. With the RPP present (solid curves), one sees that at large spatial frequency the ideal smoothing limit is achieved, however, below a spatial frequency determined by the source divergence there is little or no smoothing.

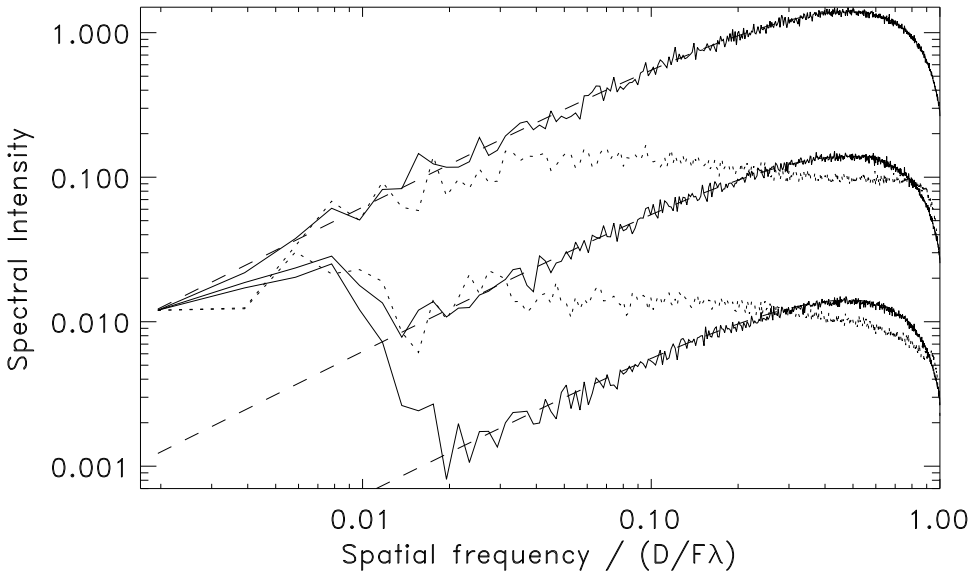

Figure 3: Comparison of calculated spatial spectra using smoothing by ISI of divergence FWHM 50 λ / D (solid curves) with that of standard FM-2D SSD of equal divergence (dotted curves) for (top to bottom) the initial static speckle pattern (for both ISI and SSD -- top solid) and after an integration time equivalent to 10 and 100 coherence times. The dashed lines show the ideal ISI smoothing result for the case of large beam divergence.

3. 2D-SSD USING FM OF A SINGLE COLOR CYCLE

The spatial spectra generated by 2D-SSD using sinusoidal phase modulation[10] are significantly different from that of ISI. For the calculation of 2D SSD, the near field is assumed to be the product of a static RPP and the time varying skewed phase modulation as shown in Fig. 1 (incommensurate FM is applied for the two orthogonal directions of 2D-SSD). In Fig. 3 the spatial spectra produced by 2D-SSD using FM with a single color cycle in each dispersion direction (i.e. where the temporal skew of the grating is equal to the modulator period; dotted curves) are shown and compared with the results of the ISI random smoothing of Fig. 2 (solid curves), where both smoothing methods are chosen to generate the same beam divergence FWHM (note that the angular spectrum of the FM-SSD beam has a rectangular shape peaked at the ends, characteristic of a FM spectrum, whereas the ISI smoothing described here has an angular spectrum of Gaussian shape).

The top solid curve is the static speckle spectrum applicable to both SSD and ISI, and the next lower solid curve (ISI) and dotted curve (SSD) are the results after integration for 10 coherence times. One sees that FM-SSD (unless otherwise specified SSD shall refer to 2D-SSD) smoothes comparatively poorly at low spatial frequency. At both integration times shown the FM-SSD spectral intensity is seen to be slightly smaller than that of the ISI smoothing at high spatial frequency, but crosses over near $0.25 f_0$. At spatial frequencies ~$0.02\ f_0$ - $0.06\ f_0$ the FM-SSD spectral intensity is 5-10 times larger than that produced by the ISI method. This band of low spatial frequencies (l-modes of 30-100) is particularly important with regard to direct drive hydrodynamic stability.[11,17] Although in the asymptotic long integration time limit ISI and SSD differ in their aggregate variance levels, it should be noted that at the times shown in Fig. 3, the aggregate variance for ISI and SSD are equal.

4. SSD WITH RANDOM PHASE MODULATION

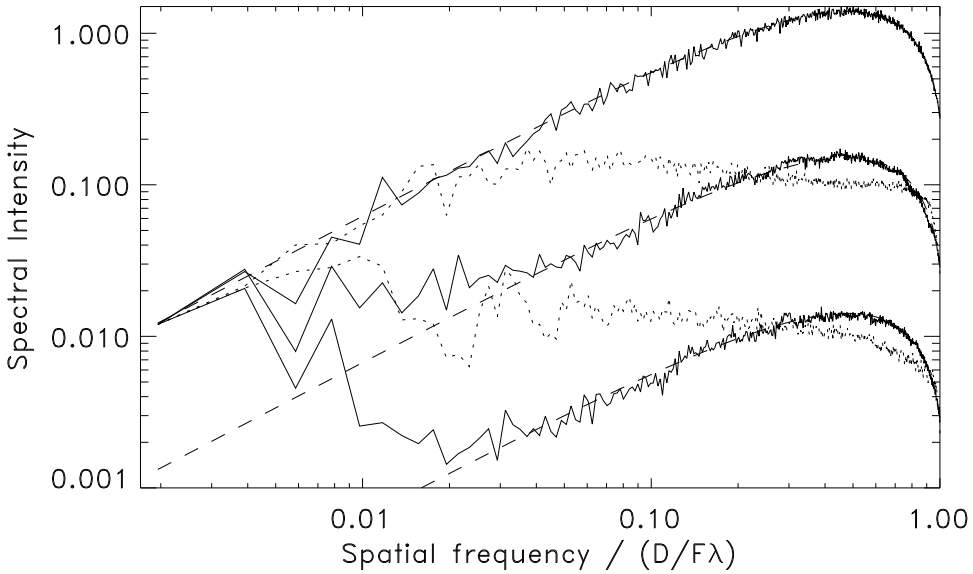

Figure 4: Comparison of calculated spatial spectra using 2D SSD with random phase modulation of ~14 color cycles across the beam (solid curves) and single color cycle FM (dotted curves) of equal beam divergence for (top to bottom) the initial static speckle pattern (solid) and after an integration time equivalent to 10 and 100 coherence times. The dashed curves show the ideal ISI smoothing result using large beam divergence.

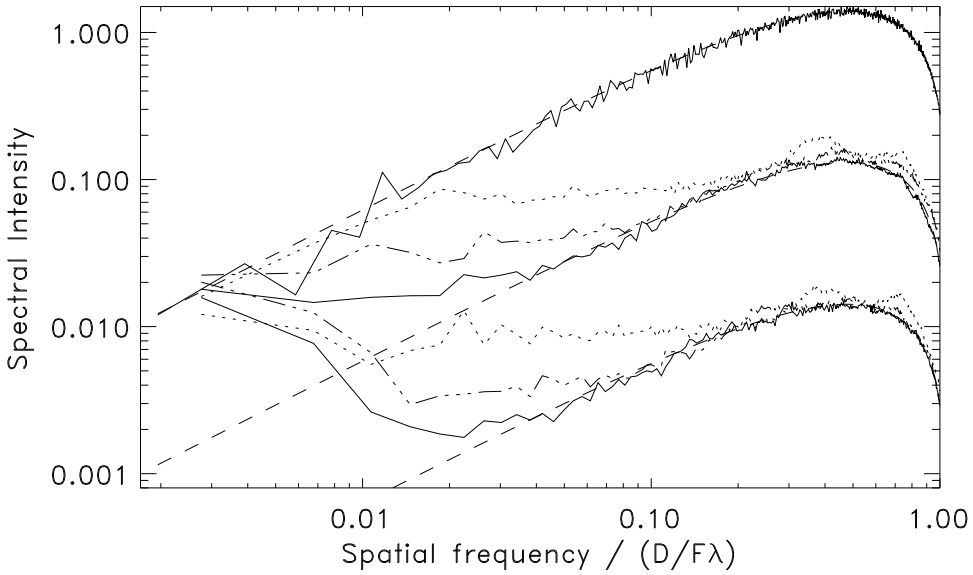

Figure 5: Comparison of spatial spectra obtained with SSD using random phase modulation with 14 (solid curves), 6.8 (dash-dot curves) and 2.7 (dotted curves) color cycles, for (top to bottom) the initial static speckle pattern (solid) and after an integration time equivalent to 10 and 100 coherence times. The beam divergence in each calculation is $50\lambda / D$. The dashed curves show the ideal ISI smoothing result using large beam divergence.

As first noted in ref. 6, the relatively poor smoothing rate of FM-SSD at low spatial frequency can be improved by increasing the number of color cycles across the beam. The number of color cycles across the beam N_{cc} is defined as the number of FM periods (T_{mod}) in the total time skew provided by the grating (T_{skew})

$$N_{cc} = T_{skew} / T_{\mathrm{mod}} = T_{skew} \cdot \nu_{\mathrm{mod}} \ , \qquad (1)$$

where ν_{mod} is the modulation frequency. By randomizing the phase modulation such that, on average, there are still many color cycles across the beam, rapid smoothing at low spatial frequency can be obtained without the presence of coherent resonances in the spatial spectrum. Since RPM can not be described by a single frequency modulation, the length of a color cycle is given by the mean phase oscillation period or the phase correlation length across the beam. The mean number of color cycles across the beam is given by the bandwidth of the phase ($\phi(t)$, as opposed to the bandwidth of the field $E(t)$) multiplied by the temporal skew across the beam, $\overline{N}_{cc} = \Delta\nu_{phase} \cdot T_{skew}$.

Figure 4 shows the spatial spectra of 2D-SSD using random phase modulation (RPM), where the RPM is simulated by filtering the white noise spectrum of a random binary sequence with a Gaussian shaped filter. In this calculation, the FWHM of the phase spectrum is taken to be

50 GHz and the phase depth is chosen to have an RMS of 3.75 rad, which results in a total bandwidth of 185 GHz for each direction of the 2D-SSD. The grating skew is taken to be 280 ps so that the mean number of color cycles is ~14 (since the mean period of the phase modulation is ~1/50 GHz = 20 ps) and after dispersion the beam has a Gaussian angular spread of FWHM $50\lambda / D$. The target illumination is calculated from the Fourier Transform of the product of the RPP transmission and the RPM field of uniform amplitude and skewed random phase $\phi(t - sx)$. The spatial spectra produced by SSD using RPM (solid curves) is compared in Fig. 4 with SSD using FM of a single color cycle (dotted curves), where the beam divergence FWHM of the two methods is equal. One sees that the RPM-SSD method generates essentially the same spatial spectra as that of the ISI method of equal divergence.

Fig. 5 compares the results of smoothing using RPM for three different values of the mean number of color cycles (2.7, 6.8, and 14), and where the bandwidth and divergence ($50\lambda / D$) are kept constant. One can see that as the number of color cycles is increased the smoothing obtained at low spatial frequency is more rapid. With 14 color cycles RPM-SSD yields equivalent smoothing to the ISI method of the same divergence. At the other extreme, in the limit of a single color cycle, RPM gives results which are similar to that obtained with pure FM of a single color cycle.

5. SMOOTHING RATE DEPENDENCE ON COLOR CYCLING

It has been previously noted that color cycling can impact the relative smoothing rate as a function of spatial frequency.[6] To obtain a detailed understanding of this smoothing rate dependence consider sinusoidal FM with N_{cc} color cycles across the beam. The SSD phase modulation in the near field can be written[6]

$$E(x) = \exp\{i\beta \sin(k_x x - \omega_{\mathrm{mod}} t)\} \tag{2}$$

where, $k_x = 2\pi N_{cc} / D$, $\omega_{\mathrm{mod}} = 2\pi\nu_{\mathrm{mod}}$ is the angular modulation frequency, and the y dependence has been omitted for simplicity but is analogous (in the case of 2D SSD).[7,10] One can find the smoothing rate at a given spatial frequency f by calculating the interference between the field at points with the corresponding near field separation $\Delta x = f\lambda F$. The intensity owing to interference of near field points separated by Δx is given by

$$\begin{aligned} E(x)E^{*}(x+\Delta x) &= \exp\{i\beta[\sin(k_x x - \omega_{\mathrm{mod}} t) - \sin(k_x(x+\Delta x) - \omega_{\mathrm{mod}} t)]\} \\ &= \exp\{-i2\beta \sin(k_x \Delta x / 2)\cos(k_x(x + \Delta x/2) - \omega_{\mathrm{mod}} t)\} \end{aligned} \tag{3}$$

This interference term is recognized as having the same form as FM with the effective modulation depth given by $\beta_{eff}(f) = 2\beta \sin(k_x \Delta x / 2)$. Low spatial frequencies on the target correspond to small Δx, so that one can approximate $\beta_{eff}(f) \cong \beta k_x \Delta x$. The bandwidth of this interference term $(2\beta_{eff}(f)\nu_{\mathrm{mod}})$ gives the approximate effective smoothing rate at the low spatial frequency of interest

$$\Delta\nu_{eff}(f) \sim 2\beta_{eff}(f) \cdot \nu_{\mathrm{mod}} \cong 2\beta\nu_{\mathrm{mod}} \cdot 2\pi N_{cc}\Delta x / D = \Delta\nu_{tot} \cdot 2\pi N_{cc} \cdot f / f_0. \tag{4}$$

where the total bandwidth is $\Delta\nu_{tot} \equiv 2\beta\nu_{\mathrm{mod}}$. Hence, one sees that the smoothing rate at low spatial frequency increases proportionally to the number of color cycles, N_{cc}. A more precise relationship between the near field color distribution and the spatial frequency smoothing in the far field can be found directly from the expression for the far field intensity

$$I_{FF}(u,t) = \left| \Im_x \{E_{NF}(x,t)\}\big|_{u/\lambda F} \right|^2 \tag{5}$$

where $E_{NF}(x,t)$ is the near field amplitude, $\Im_x$ denotes the x-Fourier Transform, and the transform variable (i.e. the spatial frequency) is substituted for as indicated in terms of u, the far field transverse coordinate. Taking the Fourier Transform of Eq. (5) gives the spatial spectrum of the far field intensity in terms of the auto-correlation of the near field amplitude

$$\tilde{I}_{FF}(f,t) \equiv \Im_u \{I_{FF}(u,t)\} = \int_{-D/2}^{D/2-\Delta x} E_{NF}^*(x+\Delta x,t) E_{NF}(x,t) dx, \tag{6}$$

where the near field aperture is taken to be $x \in [-D/2, D/2]$. This integral now represents the sum of the interference from all points separated in the near field by the gap $\Delta x = f\lambda F$. If the far field intensity is now integrated over some time interval $[0,T]$, one obtains the spatial spectrum of the fluence

$$\tilde{U}_{FF}(f,T) \equiv \int_0^T \tilde{I}_{FF}(f,t) dt = \int_0^T \left(\int_{-D/2}^{D/2-f\lambda F} E_{NF}^*(x+f\lambda F,t) E_{NF}(x,t) dx \right) dt \tag{7}$$

As explained above, one obtains smoothing because this time integral is reduced by the cancellation owing to the rapidly varying interference term in the integrand. To quantify this effect one writes the near field amplitude $E_{NF}(x,t)$ as the product of the SSD phase modulation, $E(x,t)$ given in Eq. (2), and the random phase plate transmission $R(x)$. With this substitution and upon interchanging the order of integration one obtains that the power spectrum of the fluence is given by

$$\left|\tilde{U}_{FF}(f,T)\right|^2 = \left| \int_{-D/2}^{D/2-f\lambda F} R^*(x+f\lambda F) R(x) \left(\int_0^T E^*(x+f\lambda F,t) E(x,t) dt \right) dx \right|^2 \tag{8}$$

If $\Delta x = f\lambda F$ is larger than the transverse scale of the phase plate variation, then $R^*(x+f\lambda F)R(x)$ is completely random and hence Gaussian statistics allows for the simplification of the random-walk sum of the x-integral in Eq. (8). Hence, excluding these coherent components at low spatial frequency, one finds that the power spectrum of the smoothed speckle is given by

$$\left|\tilde{U}_{FF}(f,T)\right|^2 = \int_{-D/2}^{D/2-f\lambda F} \left| \int_0^T E^*(x+f\lambda F,t) E(x,t) dt \right|^2 dx \tag{9}$$

Thus, one sees that the smoothing at given spatial frequency f is determined by the average over the aperture of the time integral of the interference between points in the near field separated by $f\lambda F$. With the substitution of interference term given by Eq. (3), one obtains

$$\left|\tilde{U}_{FF}(f,T)\right|^2 = \int_{-D/2}^{D/2-f\lambda F} \left| \int_0^T \exp\left[-i\beta_{eff}(f)\cos(k_x(x+f\lambda F/2) - \omega_{\mathrm{mod}} t)\right] dt \right|^2 dx, \tag{10}$$

where, as before, the effective modulation depth of the FM in the integrand is given by $\beta_{eff}(f) \equiv 2\beta \sin(k_x f\lambda F/2) = 2\beta \sin(\pi N_{cc} f / f_0)$. This result is exact for the 1D-SSD modulation given by Eq. (2), and is independent of the precise form of the phase plate (within the approximation of Gaussian statistics).

6. SSD USING MULTIPLE FREQUENCY MODULATION IN SERIES

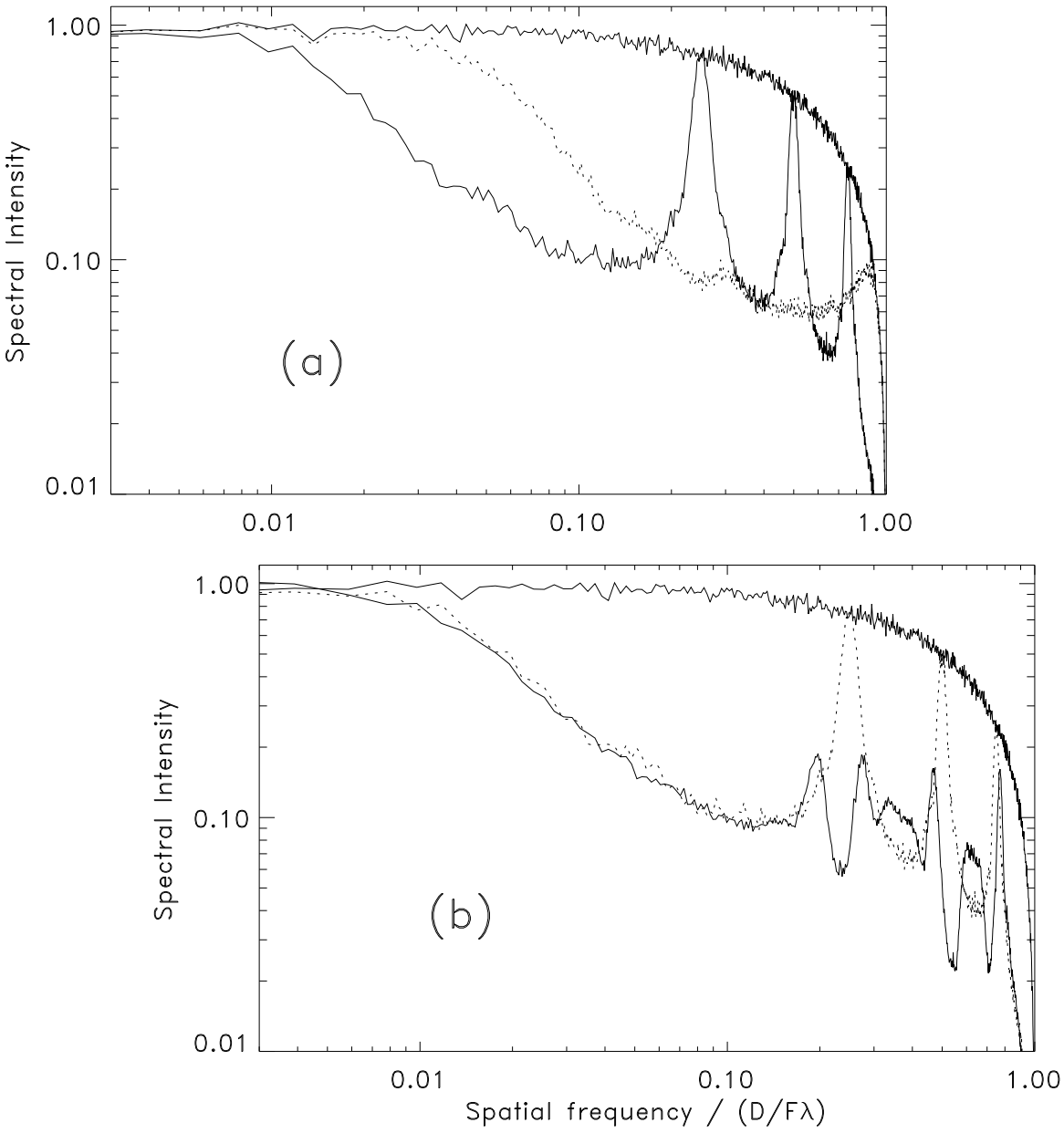

Figure 6 (a): Spatial spectra of 1D SSD with FM of a single color cycle (dotted curve) and four color cycles (lower solid curve) of equal bandwidth and divergence after an integration time equivalent to 4 coherence times. 6 (b): Spatial spectra of 1D SSD with FM of four color cycles (dotted curve, as in (a)), and then modified with the superposition of an additional FM (still 1D-SSD) of a single color cycle of equal bandwidth (lower solid curve). The upper solid curve in both plots is the static speckle spectrum.

The behavior of 1D-SSD with multiple color cycles is shown in the calculation of Fig. 6(a), where the spatial spectrum of smoothing after ~ 4 coherence times using FM with one color

cycle (dots) is compared with that of FM using 4 color cycles (solid). For clarity of the coherent resonances, these spectra are integrated orthogonally to the dispersion direction and plotted versus the spatial frequency along the dispersion direction. One sees that the smoothing at low spatial frequency is more effective when using four color cycles as predicted by Eq. (9). However, the effect of the coherence between the periodic color cycles is also readily apparent. From Eq. (8) one sees that these resonances occur when $\sin(k_x \Delta x / 2) = 0$, i.e. $k_x \Delta x = 2m\pi$ or $\Delta x = D \cdot m / N_{cc}$ (where m is an integer). At these separations the near field time variation is identical and the perfect coherence results in zero smoothing at the corresponding spatial frequencies given by $f_0 \cdot m / N_{cc}$.

Since this effect is a result of the particular periodic coherence of pure sinusoidal FM, the superposition of additional phase modulation may serve to wash out these resonances. In the calculation of Fig. 6 (b) 1D-SSD using FM of four color cycles is supplemented by the superposition of FM of a single color cycle (i.e. FM at 1/4 the frequency of the first modulator) and equal bandwidth (four times the modulation depth of the first modulator). One sees that the resonances are strongly reduced by the additional FM. Of course, in the limit of the superposition of many FM's one simply reproduces the effect of RPM. However, by proper choice of a small number of multiple FM's one may be able to obtain effective smoothing at low spatial frequency while minimizing the coherence resonances.

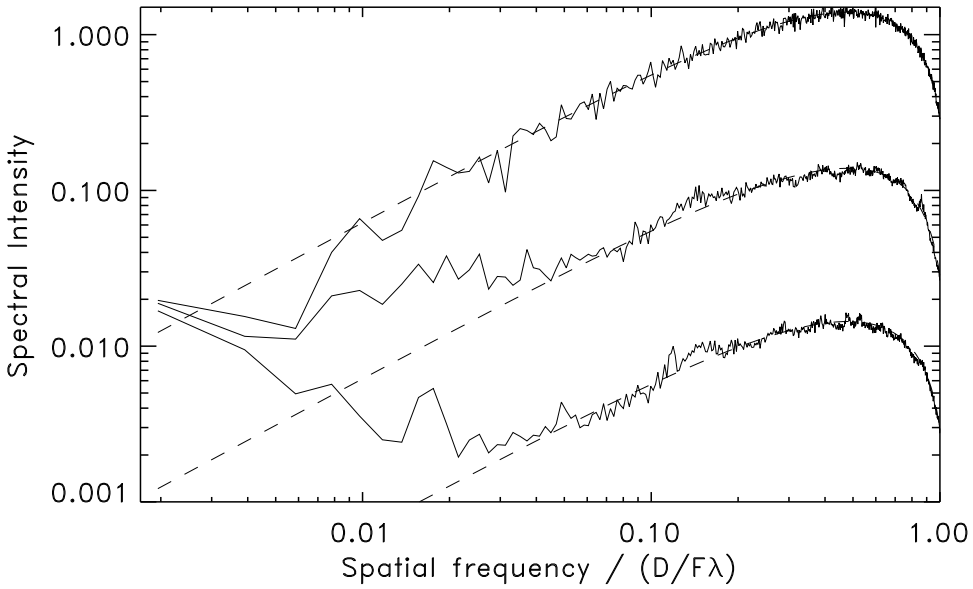

Figure 7: Comparison of spatial spectra obtained using three FM's in series for each direction of 2D SSD, for (top to bottom) the initial static speckle pattern and after an integration time equivalent to 10 and 100 coherence times (solid curves). For each direction the modulation frequencies and dispersion were chosen such that the three FM's generated 6, 4, and 1 color cycles at modulation depths of 2.7, 2.7, and 16, respectively. The induced beam divergence in each calculation is $50\lambda / D$. The dashed curves show the ideal ISI smoothing result using large beam divergence and equivalent bandwidth.

The use of multiple FM's in series is examined further in the calculation shown in Fig. 7, where 2D-SSD is implemented with 3 FM's in series in each direction. In the first dispersion direction the three modulation frequencies are in the relative ratio of 6, 4, and 1, with modulation depths of 2.7, 2.7, and 16, respectively. In the orthogonal direction all the frequencies are reduced by the factor 0.6 and the modulation depths are unchanged. For each direction the dispersion is chosen such that the three FM's generate 6, 4, and 1 color cycles, respectively. The resulting total divergence FWHM in each direction is the same as that used in the previous calculations ($50\lambda / D$). From this calculation one sees that the spatial spectra at the two integration times shown approach the results obtained with ISI at an equivalent divergence and bandwidth. In these spectra one can notice only very small effects of the resonances owing to coherence, as the interference among the multiple FM's has to a large extent washed out these resonances.

7. CONCLUSIONS

It has been shown that SSD using FM of a single color cycle is ineffective in the smoothing of low spatial frequencies. Since the smoothing performance at low spatial frequencies may be of significance for both the direct and indirect drive approaches to ICF, it is important to examine methods which improve the smoothing rate at these low spatial frequencies. It has been shown that the SSD smoothing rate at low spatial frequencies is proportional to the (mean) number of color cycles of the phase modulation across the beam. However, the use of a single sinusoidal FM of many color cycles leads to coherent resonances in the spatial spectrum. These resonances can be eliminated by either using RPM or multiple FM's. The smoothing performance of SSD using RPM or multiple FM's is then equivalent to that obtained with an ISI-type method with RPP present, where equal beam divergence and bandwidth are used.

8. ACKNOWLEDGMENT

This work was performed under the auspices of the U. S. Department of Energy by Lawrence Livermore National Laboratory under Contract No. W-7405-Eng-48.

9. REFERENCES

1. J. D. Kilkenny, S. G. Glendinning, S. W. Haan, B. A. Hammel, J. D. Lindl, D. Munro, B. A. Remington, S. V. Wber, J. P. Knauer, and C. P. Verdon, "A review of the ablative stabilization of the Rayleigh-Taylor instability in regimes relevant to inertial confinement fusion," Phys. Plasmas **1**, 1379-1389 (1994).
2. R. H. Lehmberg and S. P. Obenschain, "Use of induced spatial incoherence for uniform illumination of laser fusion targets," Optics Comm. **46**, 27-31 (1983).
3. Y. Kato, K. Mima, N. Miyanaga, S. Arinaga, Y. Kitagawa, M. Naktsuka, and C. Yamanka, "Random phasing of high-power lasers for uniiform traget acceleration and plasma instability suppression," Phys. Rev. Lett. **53**, 1057-1060 (1984).
4. R. H. Lehmberg and J. Goldhar, "Use of inchoerence to produce smooth and controllable irradiation profiles with KrF fusion lasers," Fusion Technology **11**, 532-541 (1987).

5. D. Véron, H. Ayral, C. Gouedard, D. Husson, J. Lauriou, O. Martin, B. Meyer, M. Rostaing, and C. Sauteret, "Optical spatial smoothing of Nd-glass laser beam," Optics Comm. **65**, 42-45 (1988).
6. S. Skupsky, R. W. Short, T. Kessler, R. S. Craxton, S. Letzring, and J. M. Soures, "Improved laser-beam uniformity using the angular dispersion of frequency-modulated light," J. Appl. Phys. **66**, 3456-3462 (1989).
7. D. Véron, G. Thiell, C. Gouedard, "Optical smoothing of the high power PHEBUS Nd-glass laser using the multimode optical fiber technique," Optics Comm. **97**, 259-271 (1993).
8. H. Nakano, K. Tsubakimoto, N. Miyanaga, M. Nakatsuka, T. Kanabe, H. Azechi, T. Jitsuno, and S. Nakei, "Spectrally dispersed amplified spontaneous emission for improving irradiation uniformity into high power Nd:glass laser system", J. Appl. Phys. **73**, 2122-2131 (1993).
9. H. Nakano, N. Miyanaga, K. Yagi, K. Tsubakimoto, T. Kanabe, M. Nakatsuka, and S. Nakai, "Partially coherent light generated by using single and multimode optical fibers in a high-power Nd:glass laser system," Appl. Phys. Lett. **63**, 580-582 (1993).
10. R. S. Craxton and S. Skupsky, "2D SSD and polarization wedges for OMEGA and the NIF," Bull. Amer. Phys. Soc. **40**, 1826 (1995).
11. J. E. Rothenberg, D. Eimerl, M. H. Key, and S. V. Weber, "Illumination uniformity requirements for direct drive inertial confinement fusion," Proc. Soc. Photo-Opt. Instrum. Eng. **2633**, 162-169 (1995).
12. J. E. Rothenberg, "Two dimensional beam smoothing by spectral dispersion for direct drive inertial confinement fusion," Proc. Soc. Photo-Opt. Instrum. Eng. **2633**, 634-644 (1995).
13. H. T. Powell, S. N. Dixit, and M. A. Henesian, "Beam smoothing capability of the Nova Laser," Lawrence Livermore National Laboratory ICF Quarterly Report, **1** [UCRL-LR-105821-91-1], 28-38 (1990).
14. D. M. Pennington, M. A. Henesian, S. N. Dixit, H. T. Powell, C. E. Thompson, and T. L. Weiland, "Effect of bandwidth on beam smoothing and frequency conversion at the third harmonic of the Nova laser," Proc. Soc. Photo-Opt. Instrum. Eng. **1870**, 175-185 (1993).
15. O. E. Martinez, "Grating and prism compressors in the case of finite beam size," J. Opt. Soc. Am. B **3**, 929-934 (1986).
16. J. W. Goodman, "Statistical properties of laser speckle patterns", in Topics in Applied Physics, J. C. Dainty ed., vol. 9, pp. 9-46 and 63-74, Springer-Verlag, New York, 1984).
17. M. Tabak, D. H. Munro, and J. D. Lindl, "Hydrodynamic stability and the direct drive approach to laser fusion", Phys. Fluids B **2**, 1007-1014 (1990).

Technical Information Department • **Lawrence Livermore National Laboratory**
University of California • Livermore, California 94551